Lawrence Berkeley National Laboratory

Title
Consequences of a local Coincidence for a Large Array in Ice

Permalink
https://escholarship.org/uc/item/7tp3703k

Author
Stokstad, Robert G.

Publication Date
1998-05-01
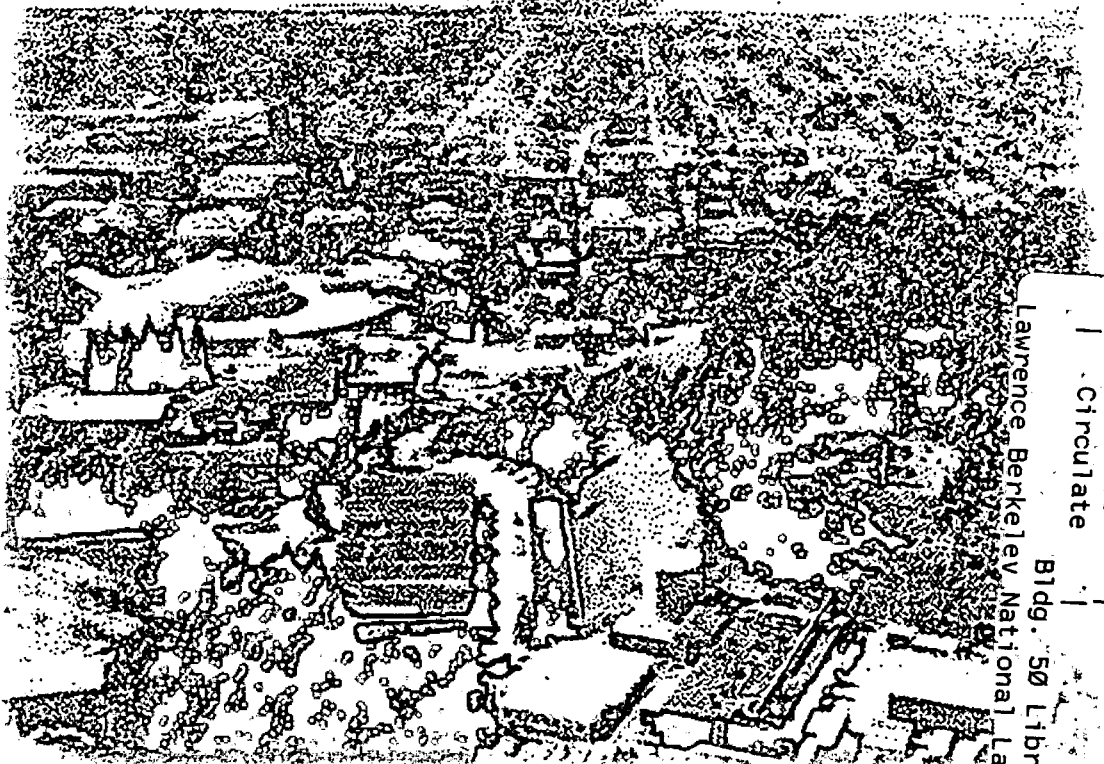
ERNEST ORLANDO LAWRENCE
BERKELEY NATIONAL LABORATORY

Consequences of a Local Coincidence for a Large Array in Ice

Robert G. Stokstad

Nuclear Science and Physics Divisions

Institute for Nuclear and Particle Astrophysics

May 1998

DISCLAIMER

Consequences of a Local Coincidence for a Large Array in Ice

Robert G. Stokstad

Institute for Nuclear and Particle Astrophysics
Nuclear Science and Physics Divisions
Lawrence Berkeley National Laboratory
University of California
Berkeley, California 94720, USA

May 1, 1998

Consequences of a Local Coincidence for a Large Array in Ice

I. Schematic Calculations Using Probability Distributions

Robert G. Stokstad

Institute for Nuclear and Particle Astrophysics
Nuclear Science and Physics Divisions
Lawrence Berkeley National Laboratory
Berkeley, California 94720

Summary

Phototubes in a Cherenkov detector, arranged on strings and located deep in polar ice or in the ocean, can be operated in a local coincidence mode in which only those tubes that are part of a "fast" coincidence contribute to an event. This greatly reduces the number of noise hits transmitted to the surface and, therefore, the bandwidth required. Not all tubes that are hit by Cherenkov photons from a muon, however, will be in coincidence with a partner. These isolated hits may have two consequences. First, there may not be the requisite number of coincidence hits to build an event or pass a subsequent software cut. Thus, there will be some loss of events or, equivalently, some reduction of the detector's effective area. Furthermore, those muons that do pass an event threshold or software cut may still have isolated hits that, unless they are recovered by a look-back process, represent lost information. This may have consequences for track reconstruction and energy determination.

We assess here some of the effects of a local coincidence for a km-sized array of optical modules (OM's) in Antarctic ice using a relatively simple method. The probability for an OM to register a hit is calculated for vertical and horizontal through-going muons having a mean energy of about 600 GeV. The distributions of hit probability versus distance are taken from Wiebusch, et al., which are based on the Monte Carlo used to predict the performance

of AMANDA-II, and are parametrized with a function introduced by Pandel. Probabilities for different coincidence modes (nearest neighbor, next-nearest neighbor, etc.) are calculated directly from the probabilities for individual OM hits. The time delay of hits due to scattering in the ice is taken into account by calculating the probability that a hit is direct, i.e., has less than 50 nanoseconds delay relative to an unscattered photon. To assess the performance of a km-scale array, we consider 5000 OM's arranged in a representative rectangular array in which the strings are spaced 100 m apart and the 50 OM's on each string are separated by $20m$. As in the present AMANDA operation, we require a minimum of 16 time-integrated (or ordinary) hits as a first level trigger and 5 direct hits for an event to pass a second-level software cut. Results are as follows: for vertical upward-going muons, the effective area for registering 5 direct hits in a next-nearest-neighbor coincidence mode is 2.1% less than the effective area for 5 direct hits without any local coincidence. The corresponding event loss for horizontal muons normal to one face of the detector is 6.5%. For horizontal or vertical muons that make this 5-direct-hit coincidence cut, there will be about 7 isolated OM's in an average total of 36 OM's.

The effects of coincidence time windows of varying length for lost events and isolated hits are studied. With an appropriate trigger threshold, a digital system incorporating a look-back to recover isolated hits should be capable of delivering essentially the same information as a system in which each OM has its own physical connection to surface.

Two appendices describe a) an evaluation of the optimum spacings between OM's and between adjacent strings for 600 GeV muons and b) effective areas for arrays of different sizes and number of OM's.

Future work on the effects of a local coincidence includes analyzing existing AMANDA B-10 data and employing a full Monte Carlo simulation of a km-scale array. In the meantime, the present schematic calculations provide encouragement for considering the use of a local coincidence as part of a first-level trigger in a very large array.

Contents

4

1. Introduction and Overview

The acquisition, transmission, and analysis of information from a remote array of optical modules (OM's) is a crucial component of the design of a km-scale high energy neutrino observatory. The range of solutions available and the optimum solution depend on a host of considerations, one of which is venue. For example, the distance from the array to the station that receives the information is a crucial parameter. In the case of ocean based detectors, this distance is sufficiently long ($\sim 15 - 40 \ km$) that the analog information from the optical modules must be digitized at the array before being sent to shore via optical fiber. At the South Pole, distances are much shorter ($\sim 2 - 3 \ km$) and it has been possible in the AMANDA project to transmit the analog information from the OM's to the receiving station above the array using an individual electrical cable (or optical fiber) for every OM. Some of the other factors that influence the choice and design of a km-scale system include the total number of OM's and scale of the array, the noise of the medium, reliability, redundancy, flexibility, the quality of the information needed, and the cost.

In all cases, the amount of data generated initially is so great that most of it will be discarded before it is eventually analyzed in detail. Photoelectrons or "hits" that are not part of an event (defined by a trigger) are eventually discarded; where and how this information is thrown away is of importance. If every pulse (whether in analog or digital form) is transmitted to the receiving station, one has maximum flexibility to define and change trigger configurations. The price is that one has to transmit all that information, most of it useless, to the surface. If the lowest level trigger is made (or the noise is eliminated) at the array, the data rate to the surface drops radically. The price however is that some useful information may be lost and that the trigger hardware below the surface has limited flexibility. These considerations weigh in the design of a system.

A local coincidence at depth is used in the Baikal detector, in which pairs of OM's placed close together are operated in a fast coincidence. Use of a local coincidence at depth has been discussed for both ocean and ice in Refs. 2-4. In ice, for example, with a noise rate of $10^3/s$, per OM and a coincidence window of 100 ns, the bandwidth required for sending data to the surface is reduced by a factor of 10^4. Reducing the noise rate for the ocean, where ^{40}K is present, is even more important.

A digital system employing a local coincidence offers certain advantages in the ice, among them large dynamic range and a reduced cost associated with fewer cables to the surface. For a very large array, the cost savings could be significant. It is not the purpose of this paper, however, to present and evaluate the relative merits of analog and digital systems

for a large array in the ice. We are motivated by a specific question that arises when noise reduction and an initial trigger take place at depth (or even on the surface) through requiring a fast coincidence among nearby optical modules.

The problem is illustrated in Figure 1, which shows the reconstruction of an up-going muon in the AMANDA B-4 array.[5] Ten OM's have recorded hits that are used in the reconstruction. Had we required that adjacent OM's be in local coincidence, the hits from nine of the OM's would satisfy this requirement and one would not. The information from that OM would, without additional steps to recover it, be lost. If we relax the coincidence requirement to include next-nearest-neighbor coincidences, all of the OM's in this particular example participate in the coincidence. Ultimately we must quantify the effects of a local coincidence on the ability to reconstruct muons (including the rejection of down-going muons), to determine their energy, and on the "effective area" of the array. How do these effects depend on the type of local coincidence we employ and on the size of the array? How important is it to develop ways to recover some of the information that otherwise would be lost?

There are three ways to answer these questions.

1. A full Monte Carlo calculation including reconstruction of events that have passed through a local coincidence requirement. This method is the most complete, as it enables simulation of a full-size, km-scale array and includes the effects of all the cuts on the data.

2. Analysis of actual data from AMANDA B-10,[6] which does not incorporate a local coincidence. One can require a local coincidence after the fact with software and evaluate the consequences. This method has the advantage of being based on real, not simulated events. It is limited, of course, to string and OM configurations that have been deployed so far.

3. Schematic calculations using probability distributions. For a muon on a given track one can calculate the probability for any single OM to be hit and, therefore, the probability for an OM to be isolated or in coincidence with a nearby OM. The hit probabilities are derived from Monte Carlo calculations incorporating the optical properties of the medium and efficiencies of the OM's. This method, while simple, incorporates most of the physics, facilitates an understanding of problem, and can be used to explore the features of arrays of any size.

All three methods are desirable and need to be pursued. We begin here with the simplest method.

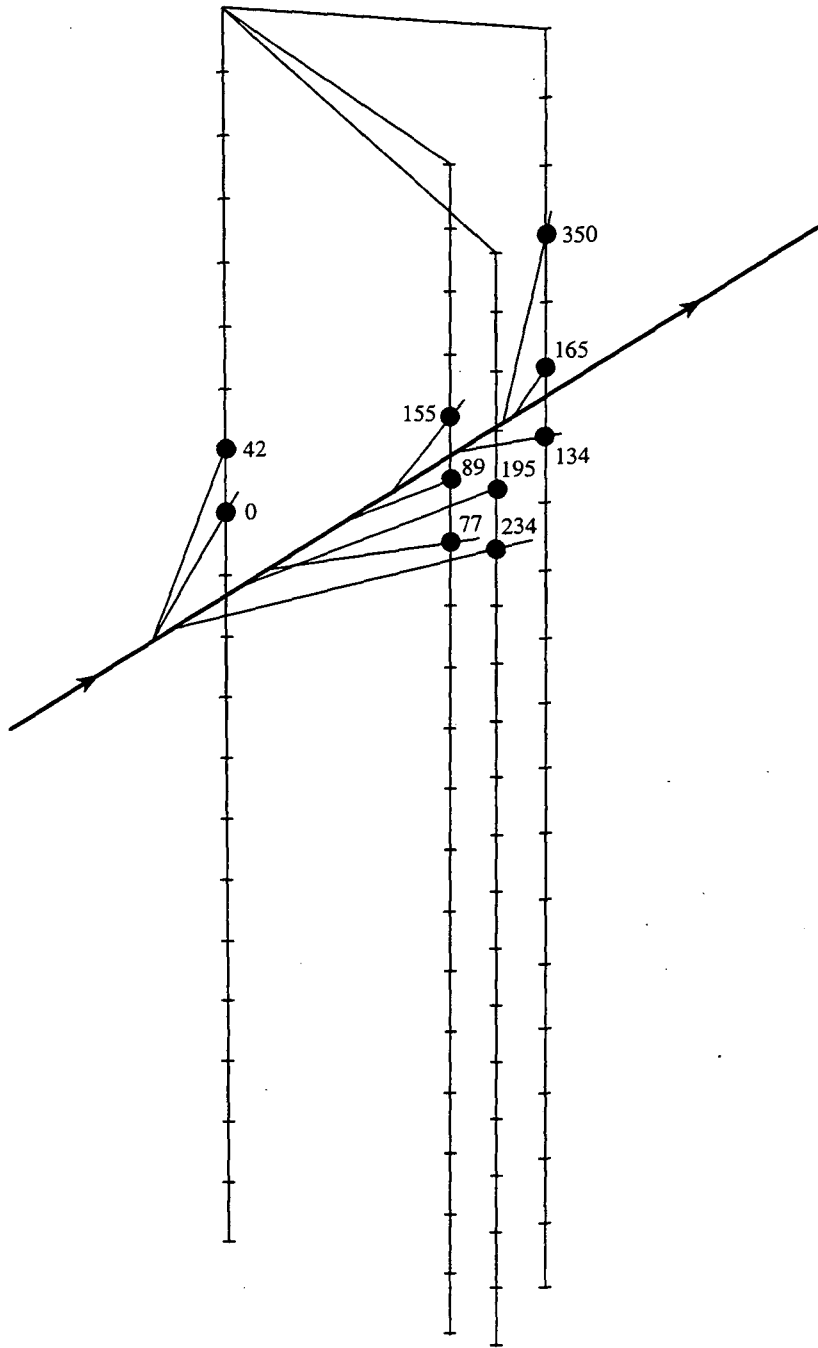The probability distributions and the function used to fit them are described in the

Figure 1: A reconstructed up-going muon event in AMANDA-B4 (from Ref. 5)

next section. Subsequent sections describe the calculation of hit probabilities for rectangular arrays and muons on different trajectories. The probability formulae for different modes or types of local coincidences and a discussion of trigger requirements complete the material necessary to present actual calculations. Much can be understood from the performance of a single string encountered by vertical and horizontal muons. Following this we consider arrays of different sizes, including a cubic km. The last section gives the conclusions of the present work and possibilities for extending these calculations in the future.

2. Probability Distributions

2.1 Advantages and limitations

The use of probability distributions derived from prior Monte Carlo calculations (as opposed to running a Monte Carlo for each case) offers the advantages of speed and simplicity. Also, the original Monte Carlo on which the distributions are based can have both high statistics and all the important physics included because that calculation, even if time consuming, is made only once. What will be missing in the present method, because it uses only probabilities, is a determination of the fluctuations that occur about the average value. Correlations among variables are also harder to treat in the present method. For the moment these deficiencies are tolerable and, in any case, will be remedied when real data or a full MC are used to examine the question of lost information.

For a muon traversing an array of OM's we calculate for each OM the probability that it will be hit, *i.e.*, that it will register one or most photoelectrons from photons emitted along that muon's track. The photons will scatter in the ice and therefore experience some delay (relative to an unscattered photon) in arriving at the OM. We determine the time-integrated probability for a hit and also the probability that the first photo electron will arrive within a certain minimum delay time, in this case 50 *ns*.

2.2 Source of hit probabilities

Sections 6 and 7 of reference 6 describe Monte Carlo simulations (tailored to AMANDA B-10 and AMANDA-II) of muon trajectories, the radiative processes associated with muon energy loss, photon propagation in ice (with appropriate scattering and absorption), and photon detection with the standard AMANDA OM. The optical parameters used in this simulation were $\lambda_s = 3.5m$ and $\langle cos\theta_s \rangle = 0.87$, which correspond to an effective scattering

length $\lambda_{eff} = 25$ m. The absorption length λ_a was wave-length dependent with a cutoff at 150 m. The average muon energy in the detector array is about 600 GeV; all muons are treated here as through-going. The probability of a hit is given in Ref. 7 as a function of the distance traveled by an unscattered Cherenkov photon from the muon track and the orientation of the PMT with respect to the Cherenkov direction. Figure 2 shows some examples of these probabilities.

2.3 Parametrization

The distributions for the time-integrated hit probability versus distance, shown in Figure 2, can be conveniently and accurately parametrized using a function derived from elementary considerations of photon transport in a medium that has scattering and absorption. More information on this function and its derivation is given in Ref. 8.

In brief, the probability that a photon at a distance r from the origin will have been delayed in its arrival by a time t is given by

$$P(r,t) = \frac{1}{\Gamma\left(\frac{r}{\lambda}\right)} \cdot \frac{1}{t} \left(\frac{t}{\tau}\right)^{\frac{r}{\lambda}} \cdot e^{-\frac{t}{\tau} - \frac{r + c_w t}{\lambda_a}} \tag{1}$$

where Γ, λ and τ are adjustable parameters related to the scattering process, c_w is the velocity of light in ice, and λ_a is the absorption length. Note that t is the time delay (due to scattering) and does not include the direct travel time, r/c_w, required for an unscattered photon to travel from the origin to point r.

2.4 Distance dependence

The time-integrated probability is

$$W(r) = \int_0^\infty P(r,t)dt = e^{-\frac{r}{\lambda_a}} \cdot \left(1 + \frac{c_w \tau}{\lambda_a}\right)^{-\frac{r}{\lambda}}. \tag{2}$$

Various extensions of the basic fit function have been made over time to suit particular purposes (Refs. 6,7). In order to include the effects of OM efficiency and orientation, the angle-dependent parameter $\epsilon(\theta)$ is introduced:

$$P_{hit} = 1 - \{1 - W(r)\}^{\epsilon(\theta)} \tag{3}$$

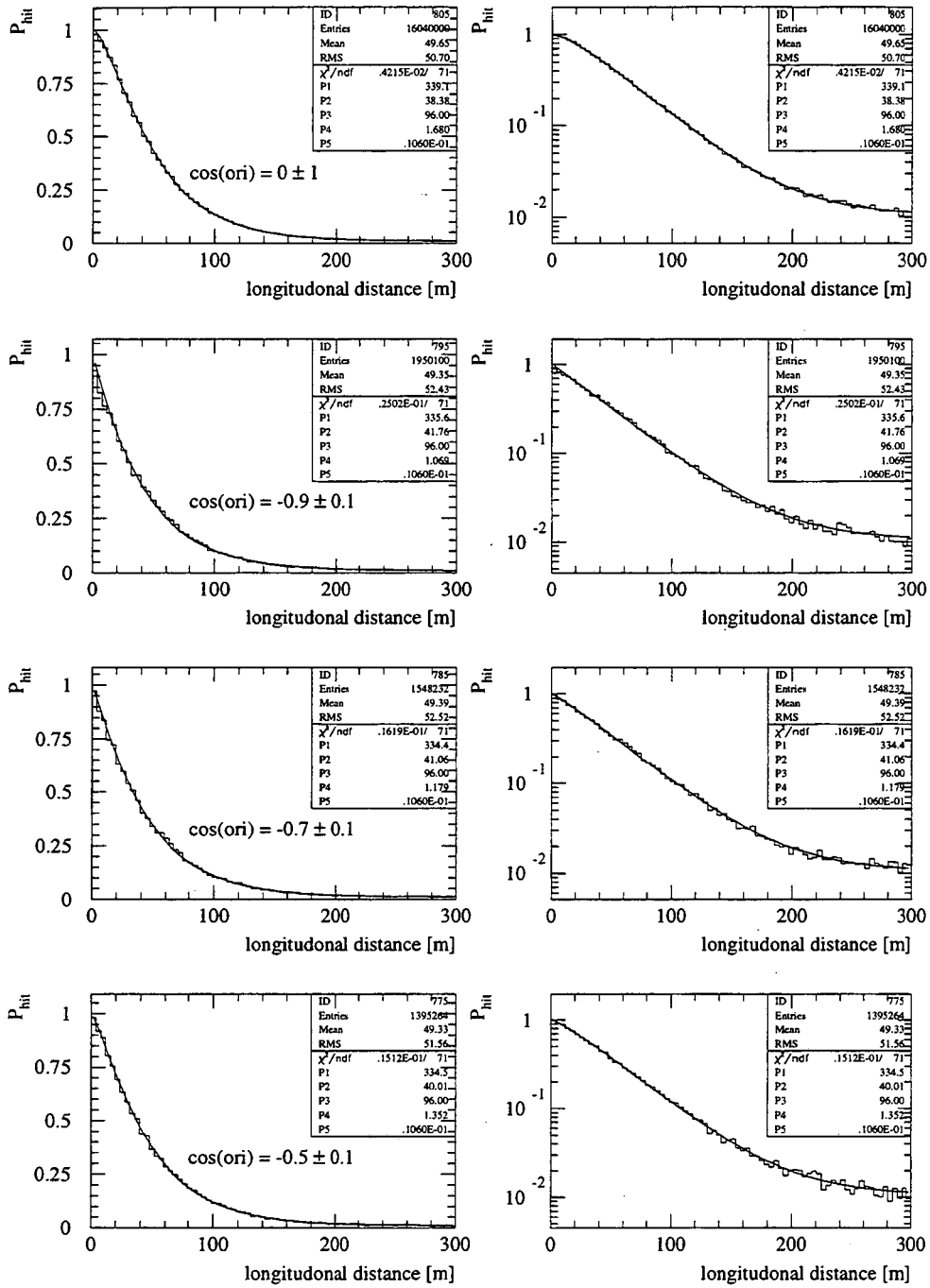where $\cos(\theta) = 1$ when the PMT points toward the Cherenkov photon.

Figure 2: Monte Carlo hit distributions. Probability vs. distance for different orientation of the phototube with respect to the direction of an unscattered Cherenkov photon. The histograms are the Monte Carlo, the full curves the fit using eqs. 2 and 3. From Ref. 7.

The parameters λ and τ are also allowed to have a θ dependence.

A term representing PMT noise can also be added. This is a small contribution, however, and we have usually set it to zero in our examination of relative rates for events with and without a local coincidence.

Figure 2 also shows the fits obtained to the MC distribution when the three parameters, λ, τ, and ϵ are allowed to depend on θ, and the absorption and noise parameters are fixed. Figure 3 shows the deduced dependence on θ. Fortunately, the parameters λ and τ describing the properties of the medium show only a relatively weak dependence on θ. We have used the values of the parameters given in Figure 3, from Ref. 7.

2.5 Time dependence

The probability that a photon will arrive at r with a time delay less than some value t can be written (Ref. 9)

$$W(r,t) = W(r)\frac{\Gamma_i(\frac{r}{\lambda}, (\frac{t}{\tau} + \frac{c_w \cdot t}{\lambda_a}))}{\Gamma(\frac{r}{\lambda}).} \tag{4}$$

In evaluating W and the incomplete gamma function, Γ_i in the above we use the same values of λ, τ, and $\lambda_a \equiv X_0$ shown in Figure 3. (The value of the parameter ϵ does not enter into the determination of the time delay.)

Figure 4 shows the differential and integral time dependence for three representative distances: 9, 25, and 49 meters. Note that the abscissa is proportional to the square root of the time. The effects of scattering on the time of arrival of photons become increasingly apparent as the source-detector distance increases.

The values of the parameters used to determine the time delay of the photons were derived by fitting the distance dependence of the time-integrated probability. Earlier experience (Refs. 6, 7) suggests that the time dependence obtained in this manner should give a reasonable reproduction of the MC, although that fit cannot be expected to be as good as for the distance dependence shown in Figure 2. It will be interesting to compare the time dependence deduced here with the MC, and it may be possible to improve the fit. In the meantime, we proceed on the assumption that our use of eq. 4 with the parameters of Figure 3 will provide an adequate estimate of the probability of an OM receiving a "direct hit," which is defined as a photon having a time delay of 50 ns or less.
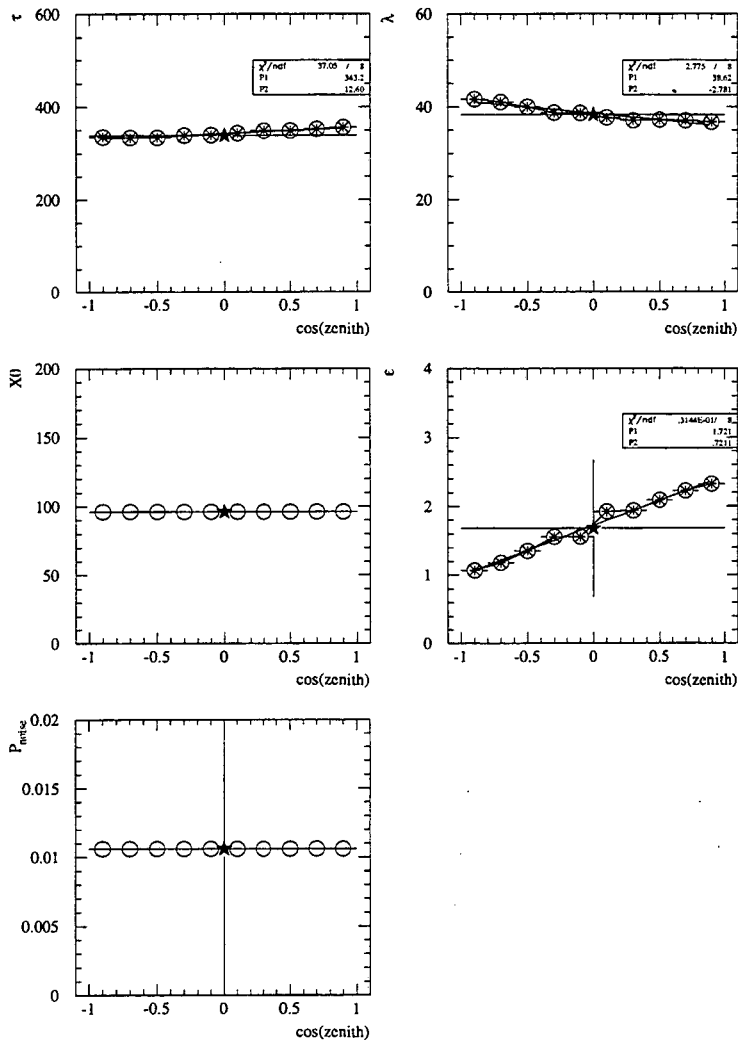
11

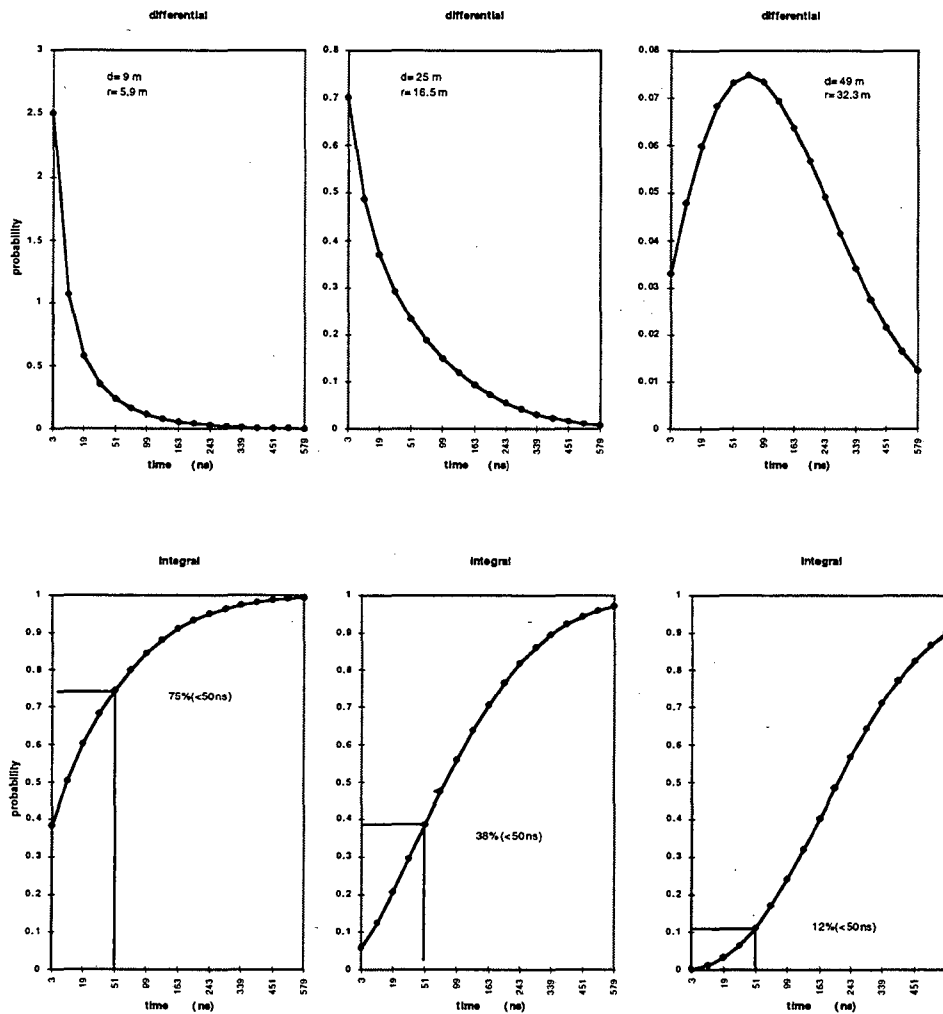Figure 3: Parameters of the (Pandel) function used to fit the distributions in Figure 2. From Ref. 7.

12

Figure 4: Hit probability vs. delay time (top row) and integral hit probability vs. delay (bottom row) calculated with eqs. 1. and 4. r is the perpendicular distance from the muon track to the OM. The abscissa is proportional to the square root of the time.

3. Hit Probabilities for Singles and Coincidence Modes

3.1 Structure of the calculation

The basic structure of the calculation consists of a through-going muon on an arbitrary straight track specified by coordinates $(x, y, z)_1$ at time t_1 and $(x, y, z)_2$ at later time t_2. The straight-line distance d travelled by a Cherenkov photon emitted by the muon and striking an OM situated at location $(x, y, z)_i$ is calculated. Given this distance and the orientation of the OM, the time-integrated hit probability is evaluated using eqs. 2 and 3. The probability that the time delay is less than 50 ns is evaluated using eqs. 2 and 4. In this manner, the time-integrated hit probability p and direct hit probability, pd, may be evaluated for every OM in an array.

The OM's are equally spaced (with separation sz meters) on vertical strings, which are themselves located on a rectangular grid, equally spaced in the x and equally spaced in the y directions. The notation is $Nx(sx)Ny(sy)Nz(sz)$: For example, 10(40m) 15(50m) 20(30m) specifies an array having 3000 OM's on 150 strings located on a 10 by 15 point grid with inter-string spacings of 40 meters along the x axis, 50 meters along the y axis, and with each string having 20 OM's located at z coordinates (from bottom to top) 0, 30, 60, ...,540, and 570 m. All OM's point down.

For a single muon on a specific trajectory, the average number of OM's in the array registering hits is $\Sigma_i p_i$, while the average number registering direct hits is $\Sigma_i pd_i$ where $pd_i = W(r_i, t = 50)p_i$ and $W(r, t)$ is the probability given by eq. 4 that a hit will arrive within t ns of an unscattered photon's arrival time.

3.2 Coincidence modes

If an array is operated in a local coincidence mode, only those OM's which participate in a local coincidence will have their hit information read out and transmitted to surface (at least initially, before any look-back occurs). For obvious practical reasons, a "fast" or local coincidence can only be taken at depth between or among OM's on the same string.

3.2.1 nearest neighbor

The probability that adjacent OM's i and $i + 1$ on the same string will both register a hit from the same muon is $p_i p_{i+1}$. We denote a nearest-neighbor coincidence mode as "two of two" or "2/2". The probability that the i'th OM will participate in a 2/2 coincidence

is $p_i [1 - (1 - p_{i-1})(1 - p_{i+1})]$. The probability that the i'th OM will have a direct hit and participate in a 2 /2 coincidence is $pd_i [1 - (1 - p_{i-1})(1 - p_{i+1})]$. There are edge effects to consider. For example, if the i'th OM in question is at the bottom of the string, this last probability changes to $pd_1 p_2$.

There are two other local coincidence modes that can be considered in a digital system.

3.2.2 next-nearest neighbor

A next-nearest-neighbor coincidence mode (2/3) occurs when any two of three adjacent OM's are in coincidence. In this mode, the data from two OM's would be sent up if they were in coincidence, even though the OM located in between them did not receive a hit. The probability for the i'th OM on a string to participate in a 2/3 coincidence event is $p_i[1 - (1 - p_{i-2})(1 - p_{i-1})(1 - p_{i+1})(1 - p_{i+2})]$. The probability that the i'th OM had a direct hit and participated in a 2/3 coincidence is obtained by replacing p_i with pd_i. The 2/3 mode is clearly less restrictive than the 2/2 mode.

3.2.3 self coincidence

An OM may also be in coincidence with itself (a mode we label 2/1) in that it may be hit by two photons (from the same muon) that either overlap in time or with some delay in between. (It is possible to design the system to recognize such events.) For example, the probability that an OM will be hit by two or more photons, with at least one of the photons arriving with less than 50 ns delay, (a direct 2/1 coincidence) is $pd_i p_i$. An interesting feature of this particular mode is that it does not require any electrical connections to adjacent OM's, at least for the purpose of making a coincidence.

3.3 Illustration

Finally, the non-coincidence or singles mode of operation is denoted 1/1 for time-integrated hits or dir(1/1) for a hit that occurs with less than 50 ns of delay due to scattering.

This nomenclature is illustrated in Figure 5, which shows a string of ten OM's, of which five are hit as a muon passes. The OM's whose data are "kept" as a result of participating in the various coincidence modes are indicated there.

These formulae, suitably adjusted for OM's at the ends of a string where partners for participation in a coincidence may be missing on one side of an OM, enable the calculation

15

Figure 5: Illustration of different coincidence modes.

of the probable number of OM's that will "send up" data when operated in any particular mode (1/1, 2/3, 2/2, 2/1) for time-integrated or direct hits.

4. Trigger levels and software cuts

There are many steps between the barrage of photo electrons ejected from the photocathodes (at a rate of $\sim N10^3 s^{-1}$, where N is the total number of OM's in the array) and the interesting few events per day of up-going muons. These steps involve successive elimination of noise, bad hits, atmospheric muons - the throwing away of unwanted bits - until only the gold-plated events of interest remain.

4.1 The AMANDA trigger

A lowest level, or level 1 trigger is the first of many sieves through which good data must pass. At present in AMANDA that trigger is located on surface and consists of a majority logic. If n tubes in the array of some 300 OM's receive hits within a certain time window t, all OM's are read out and the event saved for further analysis. Typically, $n = 16$ and $t = 5$ microseconds, corresponding to the time it takes a muon to traverse the array. Subsequent or higher level triggers often occur through software and are more aptly called cuts or filters. For example, one may require that the hits be distributed among a number of strings, or have a certain spatial or temporal topology. One may also require that a minimum number of hits in an event be prompt or "direct." Which hits are direct can only be determined after the fact, as this must be done by fitting a muon trajectory to the hit times of the different OM's and then calculating when an unscattered photon would have arrived. (This fit might be done on line and sufficiently quickly that the results could be sent back to the array before the information becomes irretrievable. This is called a look-back.) The greater the number of direct hits, the more accurately and reliably one can reconstruct the muon track. Thus, in fitting AMANDA B-4 and B-10 data, a minimum requirement of five direct hits has been set for further analysis of an event. This is quite natural, as five OM arrival times is also the minimum number required to specify a track. This cut on the number of direct hits was found (Ref. 6.) to be the most important and powerful of the software cuts applied to the data.

4.2 Spatial localization

As the number of OM's in an array increases, a hardware trigger more sophisticated

17

than a majority logic may be desirable to prevent overloading both the system and the experimenters with an unmanageable amount of data. In such a case, a trigger system could look for spatial clustering of hits that indicate a muon track or a localized shower. In this case, a large number of tubes that fired within the time window but that were rather uniformly distributed about the volume of the array would not pass the trigger. Thus, even if all the information from every OM is brought to the surface for analysis, it may prove advantageous to use a trigger logic that tests for local coincidences. This, of course, is what a digital system, incorporating a local coincidence at depth, does naturally: the unwanted bits are buried in the ice rather than dumped, as it were, on the counting room floor.

4.3 Direct hits

In either case, information is thrown away both at a first level (the majority coincidence on surface or a local coincidence at depth) and, later, at a second level, which we represent with the requirement of five direct hits. (In a full Monte Carlo analysis we would of course take into account all the subsequent restrictions and requirements that are imposed in analyzing the data. In the present schematic calculation, these other restrictions are lumped into the requirement of 5 direct hits.) Thus, in considering the consequences of a local coincidence, we must take into account the more restrictive level 2 trigger and determine what fraction of events that would pass level 2 are rejected at depth because they did not satisfy a level 1 local coincidence requirement. (This is the reason for our need to calculate the probability that an OM has had a direct hit.) In the following analysis, in addition to the time integrated number of hits, we will also calculate the number of direct hits that would be sent to the surface in any of the four modes of operation. The relative number of direct hits surviving coincidence modes and direct hits in the 1/1 mode will be one of the factors in assessing the consequences of taking a local coincidence. In this assessment, it will be important to distinguish between lost events and isolated hits in retained events.

5. Calculations for One String.

The results for an array and for muons of all directions can be understood better by considering first a single, isolated string and the hits recorded by its OM's for vertical and for horizontal muons.

5.1 Vertical muons

Consider a string located on the z axis and having 10 OM's, spaced 20 meters apart. For an upward going muon whose track intersects the x axis and is parallel to the z axis, the muon's x coordinate is the perpendicular distance from the track to the string (see inset in Figure 6.) The number of hits of each type is shown in Figure 6 as a

function of the muon-to-string distance, up to a maximum distance of 100 meters. The maximum number of hits for each mode, whether singles or coincidence is obviously 10, which is the number of OM's, and is achieved for a muon whose track overlaps the z axis. As the track distance increases, however, the curves in Fig 6. separate into two families - those corresponding to "ordinary" (or time-integrated) hits and those corresponding to direct hits. The probability that a hit will be direct decreases rapidly as the distance to the OM's increases, whether a local coincidence is required or not. To illustrate this, the following table gives the muon distance for which the most probable number of hits is one, *i.e.*, on average one* of the ten OM's in the string will register a hit of that type. s denotes singles, c denotes a coincidence mode.

Table 1

Distances at which the most probable number of hits is 1. For vertical muons and a string with 10 OM's

singles or coinc.	s	c	c	c	s	c	c	c
hit type	1/1	2/3	2/2	2/1	dir1/1	dir2/3	dir2/2	dir2/1
dist. (m)	78.3	60.6	53.8	47.3	27.8	27.3	26.0	24.1

In order to get, on average, a single direct hit, the muon needs to be $78.3 \, m - 27.8 \, m = 50.5 \, m$, or about 50 meters closer to the string then it would have to be for an ordinary time-integrated hit. The differences in distance are in general greater, depending on whether an event is direct or time integrated, than they are depending on whether it is a singles or a coincidence.

The table also shows one obvious consequence of requiring a coincidence - to obtain the same average number of hits, the muon must come closer to the OM's. However, once a

---

*Of course, when a coincidence of the type 2/3 or 2/2 occurs, the information from two OM's is read out. That only one hit is the probable number means that, on average, for every two muon tracks one of them will produce a coincidence made up of two OM's.
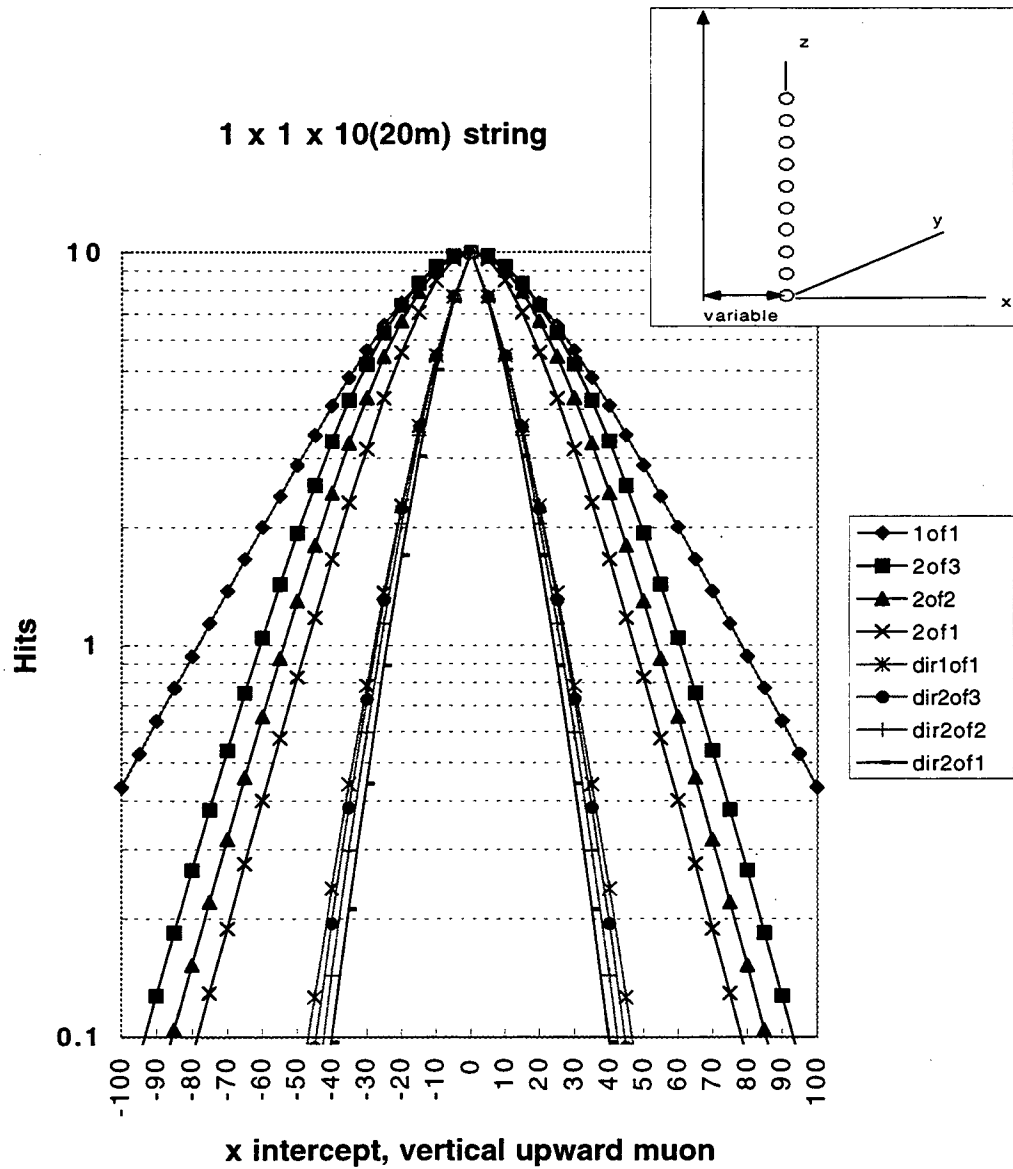
1 x 1 x 10(20m) string

Figure 6: Probable number of hits for vertical upward-going muons at different distances from a string with 10 OM's.

direct hit is also required, there is not much difference (only 0.5 m) between the distance for a dir1/1 singles and a dir2/3 coincidence. This suggests that, at least for vertical muons, the number of <u>events</u> lost due to requiring a 2/3 coincidence will be rather small, *once the level-2 requirement of direct hits is invoked.* This is an essential point.

Table 1 shows that all vertical muons passing within a distance of 27.3 m or less will produce on average 1 or more direct hits that are part of a 2/3 coincidence. If, for example, we require one hit as a threshold for an event, we must still ask how many isolated OM's there are in the events that pass this threshold. Table 2 shows the average number of hits of each type for a single vertical muon at a distance of 25 m from the string having 10 OM's.

Table 2

Hits for a vertical muon 25 m from a string with 10 OM's.

singles or coinc.	s	c	c	c	s	c	c	c
hit type	1/1	2/3	2/2	2/1	dir1/1	dir2/3	dir2/2	dir1/1
av. hits	6.52	6.25	5.44	4.25	1.36	1.31	1.14	0.89

The average total number of ordinary hits is 6.52. If we require a 2/3 coincidence, only 6.25 ordinary hits will be recorded, representing an average loss of 0.27 or 4.1% of all ordinary hits. The average loss of direct hits is 0.05 or about 3.7% of all the direct hits. These are the losses for a particular muon track. In the next section we will compute losses averaged over many parallel tracks and for an array. There is an important difference between events that are lost because they do not pass a threshold (or level 1 trigger) and isolated hits in an event that passes a threshold. Lost events are not retrievable. Isolated hits in an event may be retrieved by "looking back" immediately after the event occurs and reading out any isolated OM's before information stored in the OM is overwritten.

5.2 Horizontal muons

Figure 7 shows the case for a horizontal muon whose track is parallel to the y axis and 100 meters above the lowest OM. (Thus, if the muon intersects the string, it hits the 6th OM from the bottom.) The muon-string distance variable is the x coordinate. Comparison of Figs. 6 and 7 illustrates the basic difference or asymmetry for vertical and horizontal muons introduced by a vertical, string-type configuration and by taking coincidences only among OM's on the same string. For a given distance, the number of hits is smaller for a horizontal
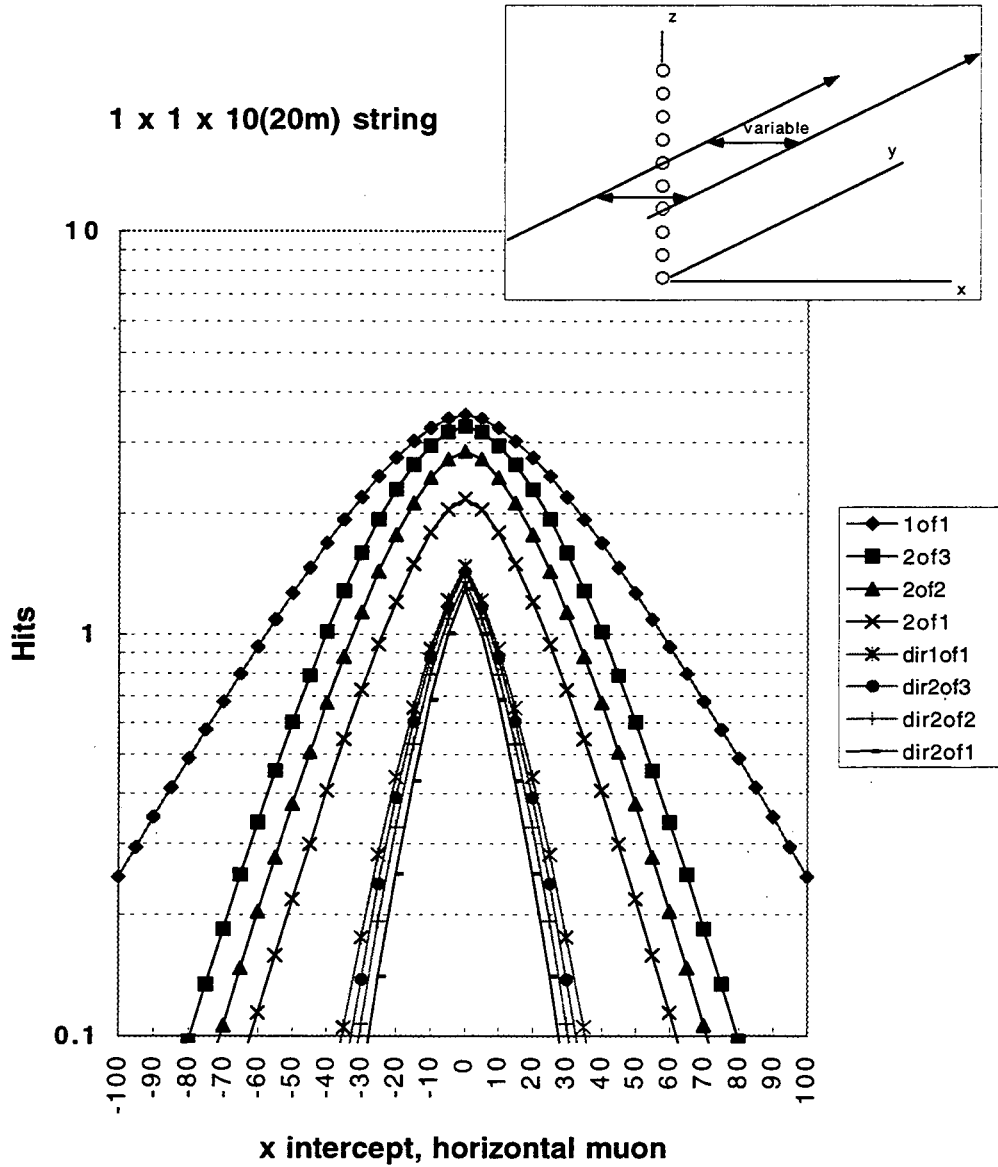
Figure 7: Probable number of hits for horizontal muons at different horizontal distances from a string with 10 OM's spaced 20 m apart.

1 x 1 x 10(20m) string

Legend:
- ◆ 1of1
- ■ 2of3
- ▲ 2of2
- ✳ 2of1
- ✳ dir1of1
- ● dir2of3
- ┼ dir2of2
- — dir2of1

Y-axis: Hits (10, 1, 0.1)

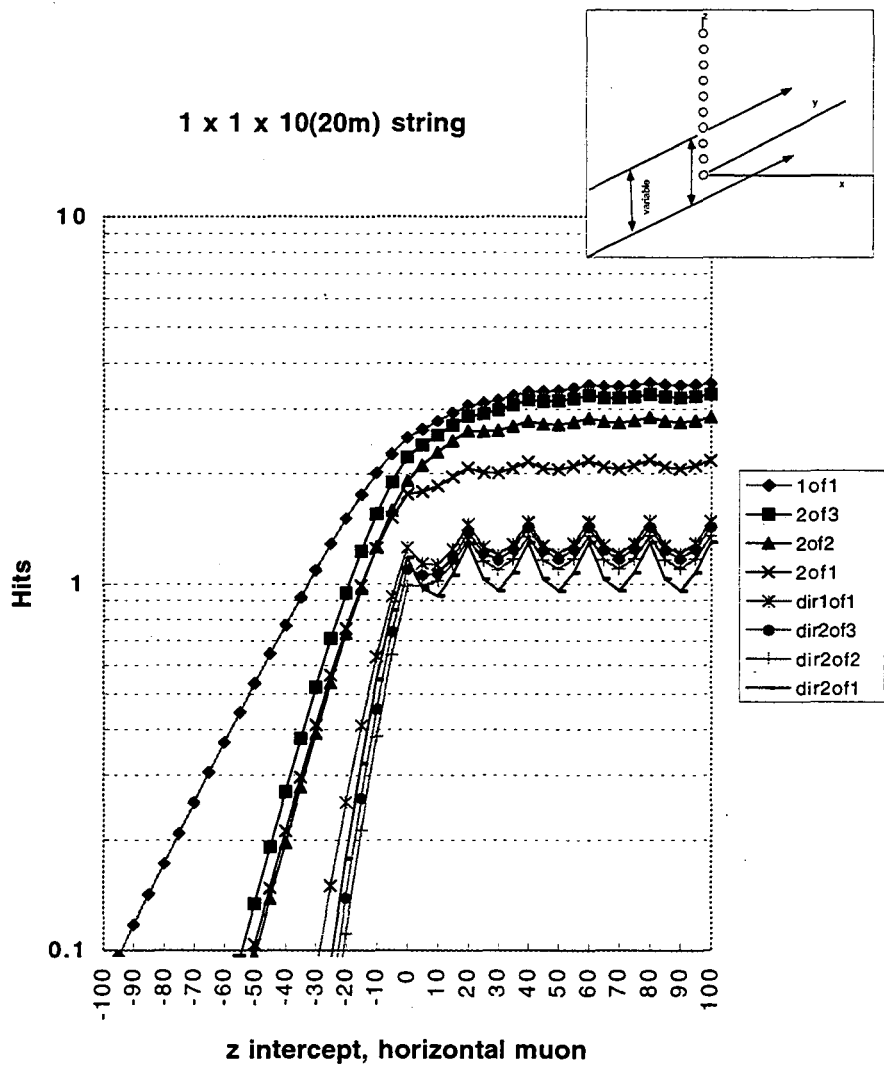X-axis: z intercept, horizontal muon (-100 to 100)

Figure 8: Probable number of hits for horizontal muons at different vertical heights along a string with 10 OM's spaced 20 m apart.

23

muon, of course, because the muon's track does not come as close to the OM's on the ends of the string. But the two families of events, ordinary and direct, also appear clustered here in Figure 7 as in Figure 6. Note that, were we to add more identical strings along the y axis, the probabilities would add linearly, because the strings are independent. Having ten such strings would simply increase the ordinate of Figure 7 by a factor of 10.

Figure 8 shows how the number of hits varies as the muon's track is fixed in the x and y coordinates (at 0,0) and is varied along the z axis. A structure, induced by the 20-meter vertical spacing of the OM's, is evident here and is more pronounced for the direct than for the ordinary events. With Figs. 7 and 8 in mind, one can have a qualitative picture of the hits that would be obtained for a horizontal muon at an arbitrary distance from the string.

Figures 6-8 thus illustrate, for a muon track at different distances from a 10-OM string, how many hits - singles or coincidence, ordinary or direct - are obtained for the extreme cases of vertical or horizontal muons.

5.3 Dependence of hit probability on the number of OM's and their spacing

The number of hits obtained will vary with the number of tubes on the string and their spacing. (However, the variation for horizontal and vertical muons will be different.) We can quantify this by defining an effective radius and calculating it as a function of the number of OM's or their spacing. The effective radius r for a certain number of hits, n, is just that distance from the string for which the probable number of hits is n. Muons with distances less than that radius will all yield more than n hits and, at larger distances, less than n hits. The effective area for obtaining n or more hits is then πr^2. Since 5 direct hits is the level-2 trigger requirement used by AMANDA in track reconstruction, we also use it for comparing singles and coincidence modes. Figure 9 shows for vertical muons the effective radii for direct hits of the type 1/2, 2/3, 2/2, and 2/1 as a function of the number of OM's on a string. (The effective radius for vertical muons is independent of the OM spacing.)

Figure 10 shows the corresponding effective areas. In Figure 10 one can see that the effective areas associated with the direct 1/1 and direct 2/3 modes are very similar, as we would expect from the numbers in Table 1. Requiring a 2/1 coincidence, however, would bring a greater loss of events.

Although the azimuthal symmetry is lacking, we can for illustration define an effective radius for horizontal muons in which we vary the horizontal distance of the muon to the center of the string, and treat that distance as a radius. See the inset of Figure 7. (In the next section we will make a proper two dimensional calculation of the effective area for

24

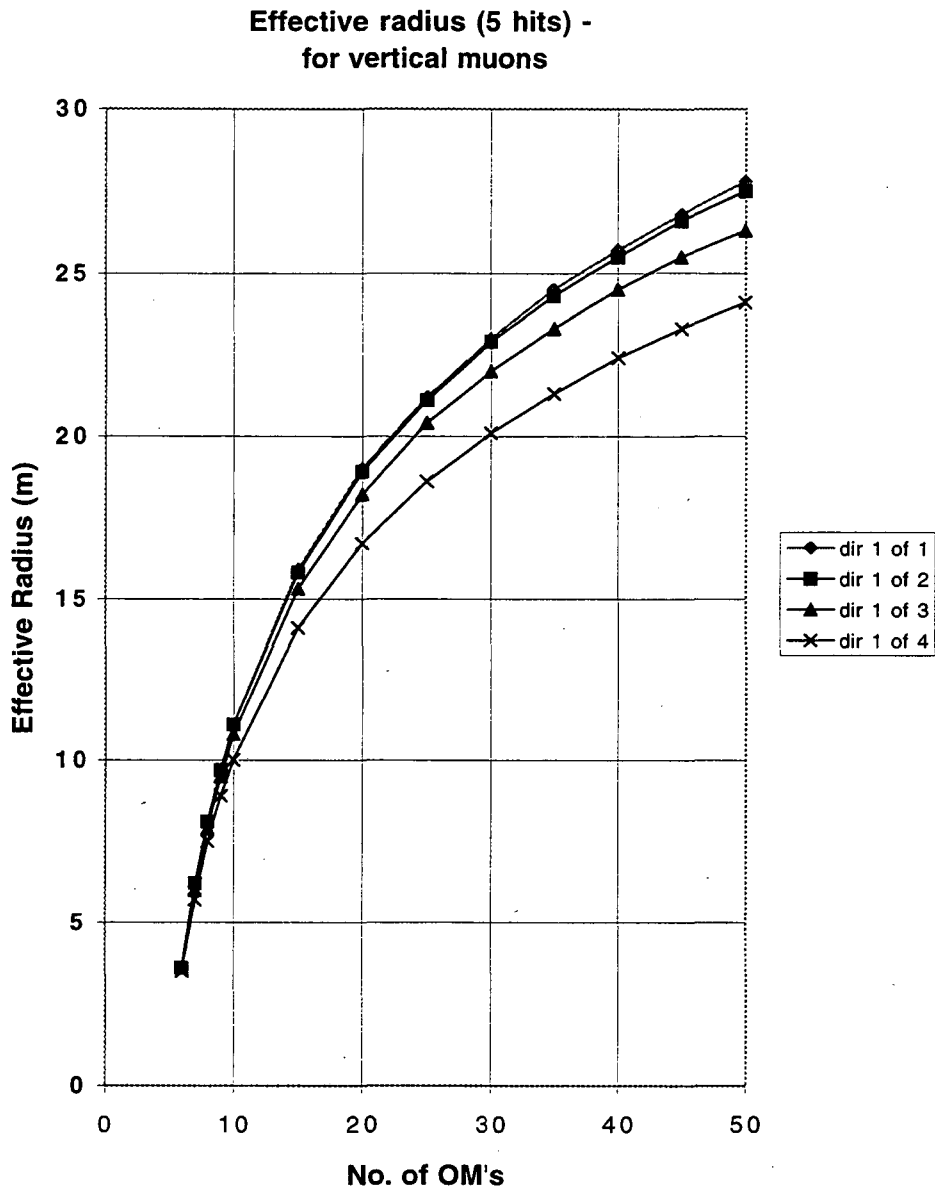**Effective radius (5 hits) -
for vertical muons**

Figure 9: The effective radius for obtaining 5 direct hits for vertical muons and a single string having different numbers of OM's.
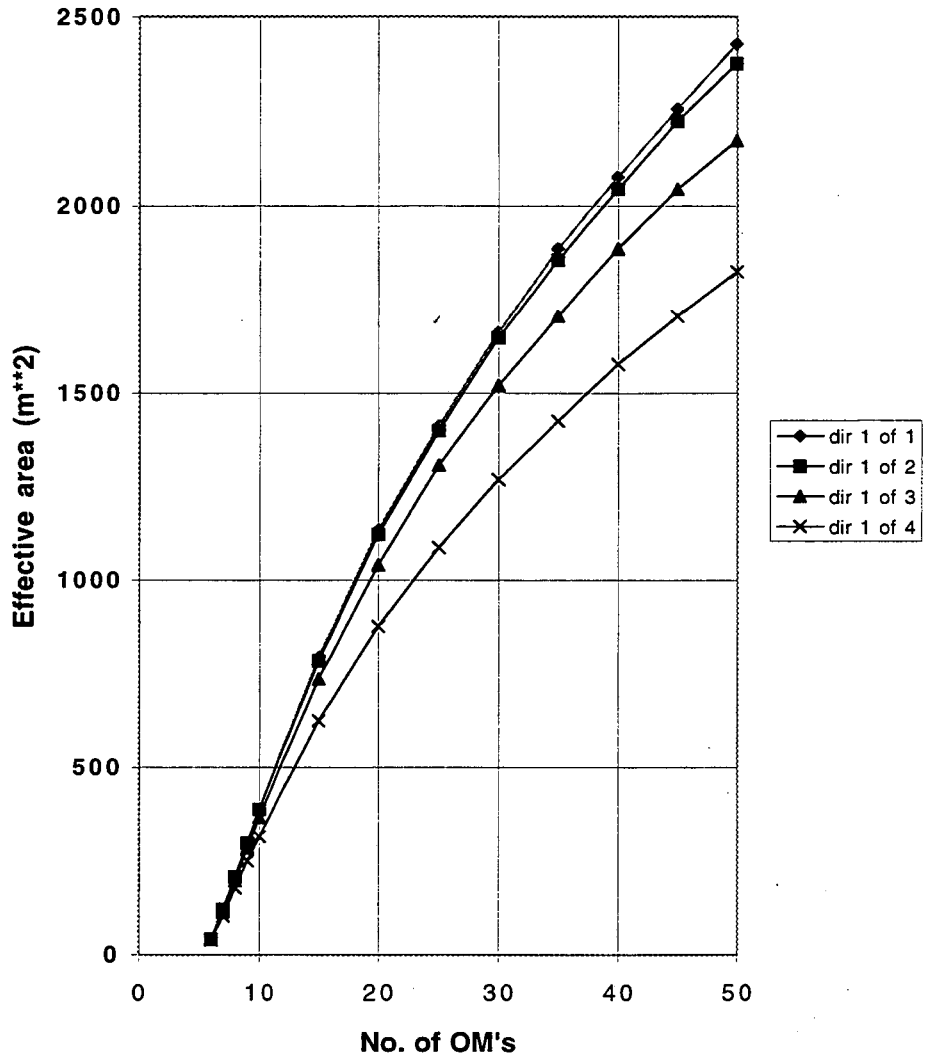
Effective area (5 hits) -
for vertical muons

Figure 10: The effective area for obtaining 5 direct hits for vertical muons and a single string having different numbers of OM's.

horizontal muons.) In this case, it is not the number of OM's which is so important - adding OM's at the ends of the string won't help much for a muon near the middle of the string - but rather the spacing of the OM's. Figure 11 shows how the effective radii for 5 direct hits varies with the spacing of the OM's. Here, the difference between dir1/1 and dir2/3 is more pronounced than in the case of the vertical muons. Also, as the spacing reaches 30 meters, the 2/1 or self-coincident mode becomes more efficient than modes requiring hits in different, widely spaced tubes.

6. Effective areas for a large array

A local coincidence coincidence becomes more important as the number of OM's in the array increases. We evaluate here the performance for a large scale array, as is envisioned for ICECUBE.

6.1 The array

A kilometer-scale detector can be simulated for our purposes by a rectangular array with the dimensions $10(100m)10(100m)50(20m)$. This 5000 OM array has a plan area of $9x9x100x100 = 0.81\ km^2$ and an elevation area (one side) of $9x100x49x20 = 0.88\ km^2$. The 100-meter spacing of the strings is not optimized for 600 GeV muons - a 50 meter spacing would be better for this energy - but 100 m is the spacing we are more likely to use, since it is better suited for the more interesting muons at higher energies.

6.2 Definition of effective area

The effective area is calculated by passing parallel muons through the array on a 1-meter by 1-meter grid. Each muon (i.e., point on the grid) that produces hits above a particular threshold contributes 1 m^2 to the effective area associated with that threshold.[†] We calculate effective areas for each mode for both a level 1 trigger of 16 ordinary hits and a level 2 software cut of 5 direct hits. We choose these values because 16 ordinary hits is the

---

[†]This definition of effective area is equivalent to the one given on p.73 of Ref. 5. $\kappa_{propogate}$ is 1.0 in our case, $\epsilon_{trigger}$ corresponds to our level 1 trigger, and ϵ_{reco} and $\epsilon_{quality}$ are subsumed in our requirement of five direct hits.

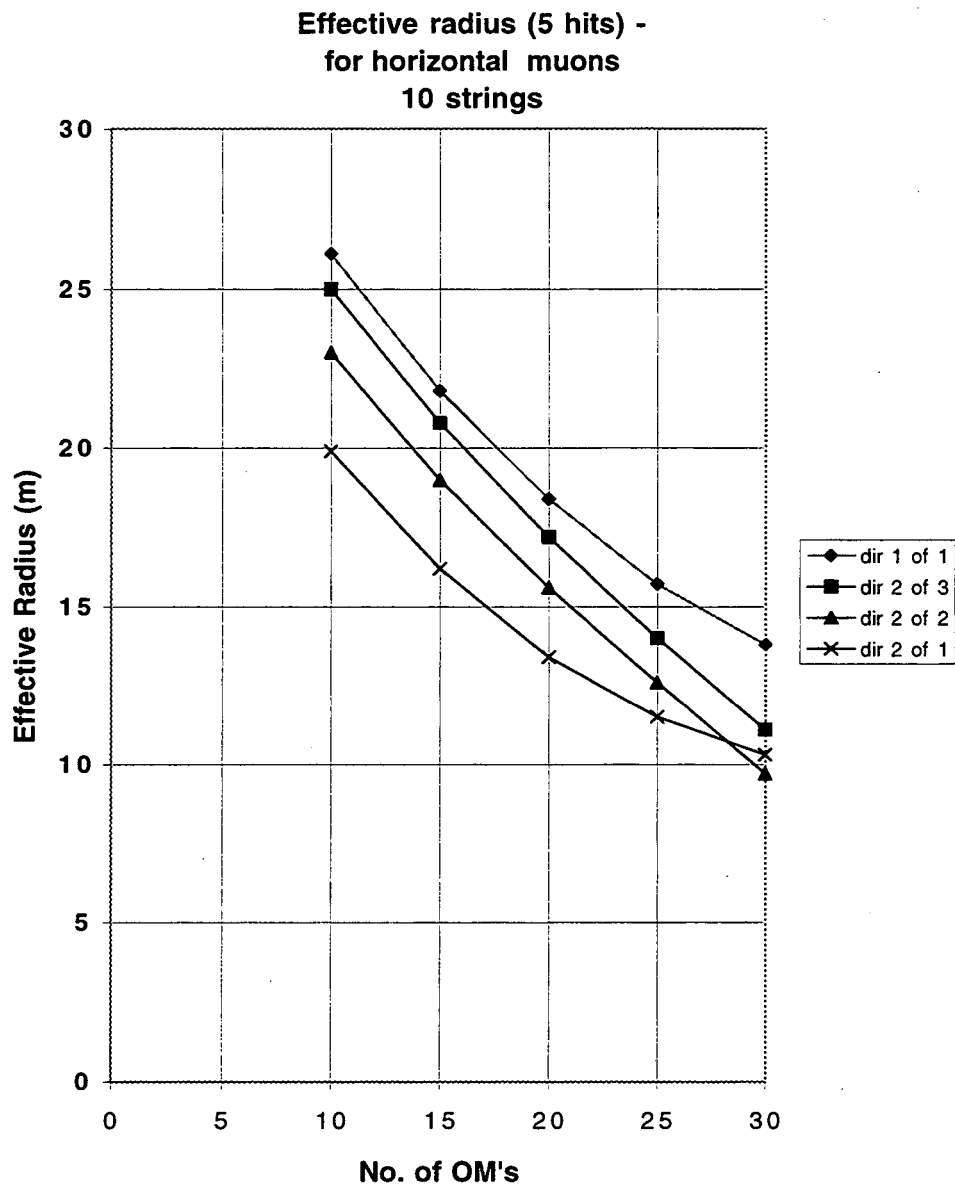**Effective radius (5 hits) - for horizontal muons 10 strings**

Figure 11: The effective radius for obtaining 5 direct hits for horizontal muons and 10 strings in a row vs. the spacing between the OM's on the strings.

majority logic trigger typically used in AMANDA B-10 and a cut on 5 direct hits is imposed in subsequent analysis. These values, 16 ordinary 8 and 5 direct, are not necessarily the values that would be used in an active array incorporating a local coincidence. But they do provide a point of comparison and answer the simple question of what would happen if we kept the present operating parameters and added a local coincidence on top of them.

The grid extends 100 meters beyond the geometric boundaries of the detector, which is a distance beyond which further extension produces negligible increase in the calculated effective area. Separate grids are used for upward, vertical muons and for horizontal muons, which are perpendicular to a face of the detector. Other orientations are possible, of course, but the extremes of horizontal and vertical muons provide a good indication of performance. To go beyond this, one should generate muon tracks having the angular distribution appropriate for down-going atmospheric muons or for isotropic upward-going muons from neutrinos.

6.3 Results: Effective areas and isolated hits

A caveat: The following results have a relative rather than an absolute significance. It is the differences between the various modes of operation (between singles and the different coincidence modes, etc.) that are most meaningful. The absolute values for effective areas given here should not be taken as predictions that would necessarily be realized by a physical detector in the ice. Such predictions are more in the realm of full Monte Carlo calculations incorporating all the necessary cuts on the data, whereas the present calculations are schematic. Thus, in cases where results are given to three significant figures, it is only so that differences among them can be taken with sufficient precision, not because their absolute values have a corresponding accuracy.

Tables 3 and 4 give the effective areas for horizontal and vertical muons. The second row of results expresses the effective area as a percentage of the geometrical area. Also included are the average number of hits obtained for each type and level of trigger or cut. *The average is taken over all muons above the threshold for that mode.*

6.3.1 Vertical muons

Table 3

Effective areas for vertical, upward muons

sing or coinc:	s	c	c	c	s	c	c	c
hit type	1/1	2/3	2/2	2/1	dir1/1	dir2/3	dir2/2	dir2/1
eff. area (km^2)	0.993	0.810	0.495	0.302	0.241	0.236	0.218	0.183
% geom.	123	100	61	37.3	29.7	29.1	26.9	22.6
av. hits.	36	28	28	28	15	15	15	15

The meaning of the values in Table 3 is illustrated by the following two examples: (i) the effective area for events in which there are $\geq$ 16 hits participating in a nearest-neighbor coincidence is 0.495 km^2, which is 61% of the geometrical area. The events above this threshold have an average of 28 nearest-neighbor coincident hits. (ii.) If we require for an event $\geq$ 5 direct hits, all of which participate in a next-nearest-neighbor coincidence, the effective area is 0.236 km^2. The average number of direct hits for events of this type is 15.

There is a 19% reduction in the effective area for ordinary hits when going from the 16 hit majority level-1 trigger (0.993) to a trigger where 16 hits are required from OM's participating in a next-nearest neighbor coincidence (0.810). Note, however, that many of the events contained in the 1/1 (or singles) trigger do not survive the subsequent requirement of five direct hits. When this level-2 requirement is introduced, the, loss in effective area in going from singles to coincidence (from dir1/1 to dir2/3) is only 2.1%.

A 50% reduction in level 1 trigger rate occurs with a nearest-neighbor coincidence (compare 1/1 and 2/2 in Table 3), and the loss in effective area at the second level trigger (comparing dir1/1 and dir2/2) is now 9.1% rather than 2.1%.

6.3.2 Horizontal muons

Table 4 gives the effective areas for horizontal muons at normal incidence to one side of the detector.

Table 4

Effective areas for horizontal muons at normal incidence to one side of the detector

sing or coinc:	s	c	c	c	s	c	c	c
hit type	1/1	2/3	2/2	2/1	dir1/1	dir2/3	dir2/2	dir2/1
area (km^2)	0.99	0.65	0.45	0.26	0.367	0.343	0.304	0.267
% geom.	112	74	51	29	41.6	38.9	34.4	30.3
av. hits.	31	25	23	19	9.3	9.1	8.8	8.2

For horizontal muons the decreases in effective areas in going from 1/1 (singles) to 2/3 (coincidence) are 34% for ordinary hits and 6.5% for direct hits. The 6.5% loss of effective area at the level 2 trigger compares with the 17% loss if a nearest-neighbor coincidence (dir2/2) is taken.

6.3.3 Isolated hits

The losses in events and number of isolated hits are summarized as percentages in Table 5. In this table we see the desirability of a next-nearest-neighbor coincidence mode, which has significantly smaller event losses than either of the other two coincidence modes. Furthermore, a sizeable fraction of the total number of hits occurs in OM's that are isolated. If these hits, even though they tend to be late-arriving, are important for energy measurement, than their recovery by a look-back procedure is desirable.

Table 5

Summary of lost events, isolated hits for a $10(100m)10(100m)50(20m)$ array

Coinc. mode	average % of lost events[a]		average % of isolated hits[b]	
	vertical	horizontal	vertical	horizontal
dir2/3	2.1	6.5	15.5	18.6
dir2/2	9.1	17.1	21.3	31.7
dir2/1	24.0	27.2	31.1	48.6

31

a) relative to the no. of events obtained for a threshold of 5 dir1/1 hits.

b) relative to the no. of ordinary 1/1 hits obtained for all muons above a 5 direct hit threshold in the 2/3, 2/2, or 2/1 modes, respectively.

A calculation made with up-ward going muons parallel to the diagonal of the array (parallel to the line defined by points (0,0,0) and (900,900,980)) gave results generally in between those for vertical and horizontal muons, but closer to the horizontal muon values. The fraction of isolated hits, however, was somewhat larger.

7. Coincidence time windows and look-back

7.1 Coincidence time windows

The coincidence hits given in Tables 1-5 are all calculated with probabilities corresponding to time-integrated hits for all OM's involved in a coincidence or, in the case of direct hits, with a 50 ns window for the OM in question and time-integrated windows for the other OM's associated with it. This implies that the timing windows in actual coincidence circuits must be sufficiently broad to include the late-arriving scattered photons. A window of finite width will cause some loss of hits. We can use the time distribution given by eq. 4 to calculate the losses associated with finite coincidence windows. The calculation is done by replacing time integrated probabilities with ones that correspond to photons arriving with less than a certain time delay, for all OM's. That time delay is specified in Tables 6 and 7, which give results for vertical and horizontal muons. The width of a coincident window (defined as the time that an OM holds its waveform information and waits to see if a discriminator pulse arrives from a nearest neighbor) would be the sum of the electronic pulse travel time ($\sim$60 ns), the maximum difference in arrival time at the OM's for unscattered photons ($\sim$60-70 ns), and the time delay in Tables 6 and 7. The first two time intervals are doubled for a 2/3 coincidence mode.

32

Table 6

Relative effective areas for different coincidence time windows. For vertical muons.

Time[a]	2/3[b]	2/2[b]	2/1[b]	dir2/3[c]	dir2/2[c]	dir2/1[c]	isol.[d]
∞	1	1	1	1	1	1	16
2000	1	1	1	1	1	1	16
1000	.92	.92	.97	1	1	.96	16
750	.80	.83	.90	1	.98	.96	19
500	.54	.67	.74	1	.93	.96	23
250	.32	.39	.46	.93	.87	.82	35
125	.17	.21	.24	.82	.73	.64	51
75	.11	.14	.14	.74	.62	.53	60

a) time window in *ns*.

b) threshold = 16 hits

c) threshold = 5 direct hits

d) isolated hits for operation in the 2/3 coinc mode, expressed as a % of time-integrated hits for muons above the 5 direct (2/3) hit threshold.

Table 6, for vertical muons, indicates that, for time windows less than about 1000 *ns*, the number of events meeting the 16 hit criterion becomes impacted, and is substantially reduced for times less than 250 ns. These 16 hits are no longer "ordinary" but, because of the short time delay allowed, are becoming more "direct" in nature. For time windows less than 250 *ns*, the number of coincidence events meeting the criterion of 5 direct hits begins to decrease. Similar, though somewhat more severe reductions are evident in Table 7 for horizontal muons. Indeed, for times of 125 *ns* or less, no coincidence events meet the 16 hit threshold, and the direct coincidence events are reduced by 1/3 to 1/2 . Both tables show the steadily increasing percentage of isolated hits as the time window is narrowed. It is clear that, if short time windows are used, a look-back procedure to recover lost events (as well as a reduction in the number of hits required to build an event) will be required.

33

Table 7

Relative effective areas and isolated hits versus time delay windows. For horizontal muons.

Time[a]	2/3[b]	2/2[b]	2/1[b]	dir2/3[c]	dir2/2[c]	dir2/1[c]	isol.[d]
∞	1	1	1	1	1	1	19
2000	1	1	1	1	1	1	19
1000	.94	.92	.86	1	1	1	21
750	.83	.76	.86	1	1	.95	24
500	.71	.75	.63	.89	.96	.86	31
250	.40	.33	0	.88	.87	.83	48
125	0	0	0	.66	.62	.66	66
75	0	0	0	.55	.50	.52	77

a) time window in *ns*.

b) threshold 16 hits

c) threshold = 5 direct hits

d) isolated hits for operation in the 2/3 coinc mode, expressed as a % of time-integrated hits for muons above the 5 direct (2/3) hit threshold.

7.2 Look-back

Ref. 4 describes a method for retrieving isolated hits in an event. Basically, after the information comprising an event at the level 1 trigger (e.g., 16 ordinary hits within 5 microseconds) is sent to surface, it is analyzed in real time and a decision made to read out additional OM's that did not participate in the event at the level 1 trigger, but that are likely to have been hit by photons from that muon. Each OM needs to store in a buffer the history of hits over some period of time long enough for a real-time analysis to be made on surface and retrieval instructions to be sent back to the OM's. Ref. 4 indicates that this is feasible. The only reduction in the quality of the information would be that the waveform is not stored in the buffer and the time resolution is that of a coarse time stamp interval. If this interval were 30-50 *ns*, this would be adequate resolution, since the isolated hits being recovered tend to be associated with more distant muons and are therefore more likely to have scattering delays.

Once a look-back is instituted, the choice of the time delay window is less critical and it could be made shorter, since the extra isolated hits will be retrieved.

8. A "No-Loss" System

We have assessed the consequences of a local coincidence by considering the present operation of the AMANDA arrays (a 16 hit majority logic trigger) and asking what losses are incurred by adding a local coincidence, keeping everything else the same. But how would one operate an array that incorporated a local coincidence and an electronic look-back?

Under a local coincidence the rate from noise hits is essentially nil. If the local coincidence window is set broadly, say 1 microsecond, to accommodate delayed photons, the random rate per tube is the order of $10^3 x 10^3 x 2 x 10^{-6}/s$ for nearest neighbor coincidences and twice this for next-nearest neighbor coincidences. The noise rate for 5000 OM's is thus 10 (or 20) KHz. In the 5 microseconds it takes a muon to traverse the longest dimension of the array, there will be only 0.05 (or 0.1) random coincidence hits. (Without a local coincidence, there would be 25 random hits.) It is clear that a trigger level much smaller than 16 hits can be imposed.

Lowering the trigger level from 16 to 8 hits has the following consequences:

Every muon that has a probable number of direct 1/1 hits equal to 5 or more now also has a probable number of ordinary hits that is 8 or more. This is true for both 2/3 and 2/2 coincidence modes and for coincidence window times down to 250 ns. It follows that every muon that meets the minimum criterion for analysis (5 direct 1/1 hits) now produces a level 1 trigger. A look-back will then locate every isolated hit, including any isolated direct hits. Every hit that participated in a local coincidence will have the full waveform and highest resolution time information. (If a hit involved only one photo electron, a much reduced set of pulse-shape information is retained.) The isolated hits retrieved in the look-back will not have waveform information and will have a time resolution of 30 - 50 ns, depending on the choice of the coarse time stamp interval. This resolution, however, is still sufficient to recognize a direct hit. Therefore, all direct hits, whether in coincidence with a partner OM or isolated, will be registered. Thus, no events will be lost, and all hits will be recorded. The following table gives the number of isolated hits that occur for a coincidence window of

1000 ns. The only effect of decreasing this time window is that the number of isolated hits, and therefore the number of OM's with less than full information, increases. This is shown in Table 8.

Table 8

Percentage of isolated hits for horizontal muons having $\geq$ 8 ordinary hits <u>and</u> $\geq$ 5 dir1/1 hits.

Time[a]	2/3		2/2	
	all hits[b]	dir hits[c]	all hits[b]	dir hits[c]
1000	20%	2.3%	32%	5.2%
250	48%	6.4%	54%	11%

a) time window in ns

b) average total hits = 36

c) average dir hits = 9.3

Two other important items, not a part of the present study, are:

1. The atmospheric muon event rate.

The event rate for down-going atmospheric muons could be as high as several kHz for ICEcubed. This poses another challenge for the electronic processors on surface - how to reject a sizeable fraction of these in order not to have to write all that information on tape.

2. A supernova trigger.

Since it is not possible, with a local coincidence at depth, to put 5000 channels into a majority logic circuit, a search for supernovae or GRB neutrino bursts will be made by periodically reading out scalers from individual OM's. The detailed strategy for this has yet to be developed.

9. Conclusion

An electronic system incorporating a local coincidence into a large array in the ice

requires substantially less bandwidth from the array to surface. Several types of coincidence operation are possible - self coincidence, nearest neighbor, and next nearest neighbor - with different effective areas and number of isolated hits associated with each. The performance for vertical and horizontal muons is different; vertical muons are somewhat easier to detect than horizontal. The next-nearest neighbor mode has the highest acceptance and, when included in an array operated with a "singles" trigger level (16 hits), captures typically 95% of the good events (5 direct hits) that would be detected with a majority logic and no local coincidence. Lowering the threshold (which is possible, given the low coincidence rates) and introducing a look-back to retrieve most of the information from isolated hits, eliminates these losses even when the coincidence windows are comparable to the delay times due to scattering.

The present calculations, while encouraging, are only a part of the picture. It is important to examine existing data taken with AMANDA B-10 and the first strings of AMANDA II to asses the affects of a local coincidence in a real situation. A full Monte Carlo calculation will be essential.

Appendix A. Array Optimization

The effective area of an array for muons of a given energy depends on the spacing between the OM's, on the spacing between the strings, as well as on the trigger and on the choice of coincidence mode. "Optimum" is defined here as maximizing the effective area for a fixed number of OM's distributed on a fixed number of strings. We want to illustrate the effect of the coincidence mode on the optimum spacings, and do so here for 600 GeV muons. We realize, of course, that it is unlikely that a km-scale array would be optimized for such a low energy as this but present the following results because they illustrate qualitatively the effect of the coincidence mode.

The optimum values of the spacings are determined directly by simply calculating the effective area for different spacings. We do so by changing only one parameter at a time. (An optimization with both parameters varied simultaneously would in principle be better, but it isn't really necessary here.) Thus, the optimum OM spacing is evaluated with the string spacing fixed at 50 meters. The optimum string spacing is determined with the OM spacing fixed at 20 meters. The results tend to justify the choices of these fixed spacings for determining the optimum values. In practice, only a representative portion of an array need be considered in performing the optimization. Thus, two strings with 10 OM's each were used in the calculation to determine the optimum OM spacing for horizontal muons, and four strings with 50 OM's each were used to obtain the optimum string spacing for vertical muons. The effective areas are evaluated for 5 direct hits, and a large, i.e., 1-2 microsecond coincidence time window is assumed.

Figure 12 shows how the effective area for horizontal muons varies with OM spacing. For close spacings (such as 10 meters) all muons are above threshold, and increasing the spacing increases the effective area linearly, just as the geometrical area is increased by lengthening the string. A

maximum value is reached for a spacing large enough such that a muon in a horizontal plane midway between OM's can contribute hits to rows of OM's above and below the plane and just make the threshold of, e.g., 5 direct events as it passes horizontally along the strings in a full sized array. Further increase in OM spacing causes the effective area to decline because a muon makes threshold only when it is close to one row of OM's or to another.

The OM spacing for which a maximum is reached depends on the mode of operation,
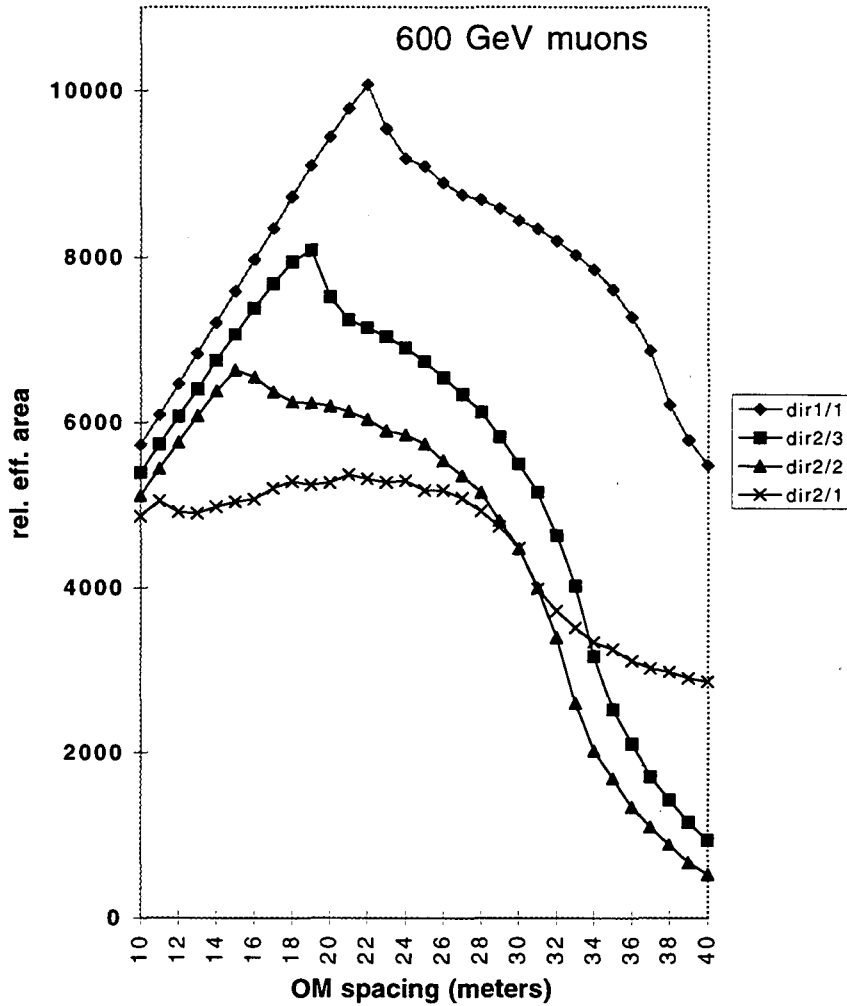
optimum OM spacing, horizontal muons

Figure 12: The relative effective area (for 5 direct hits) obtained for 600 GeV muons incident horizontally (normal to a face) vs. the spacing between the OM's on the strings. The maximum values of the respective curves indicate the optimum spacing for the different coincidence modes. The calculations were made for a fixed string spacing of 50 m.

as can be seen in Figure 12. When coincidences among adjacent phototubes are required, the maximum effective area is reached for a smaller OM spacing, as would be expected. The dir2/3 mode has its maximum at an OM spacing of 19 meters.

The dir2/1 mode, in which a single OM is in coincidence with itself, shows a quite different dependence on OM spacing. At large OM spacings, (above 30 meters) it becomes the most effective of the three coincidence modes for horizontal muons.

Similar qualitative arguments explain the dependence of effective area on the interstring spacing, which is shown in Figures 13 and 14 for horizontal and vertical muons, respectively. Though the optimum values are different for horizontal and vertical muons, a spacing of 50 meters is a good compromise value for the dir2/3 mode. Note that at large separations the effective area becomes a constant. This is the point at which, for vertical muons, only one string receives hits, and, for horizontal muons, only a few rows of OM's contribute to the event threshold.

If these calculations were performed for higher energy muons, the optimum spacings would be at larger values. An array optimized for a given energy will be less effective at lower energies because muons will not produce enough light to meet the hit requirements. The array will also be less effective at higher energies because, with more light from these higher-energy muons, the strings could have been more widely spaced and thereby increased the effective area. It is clear that the choice of the muon energy for which the array will be optimized is a critical determinant of the size of the array for a given number of strings and OM's.

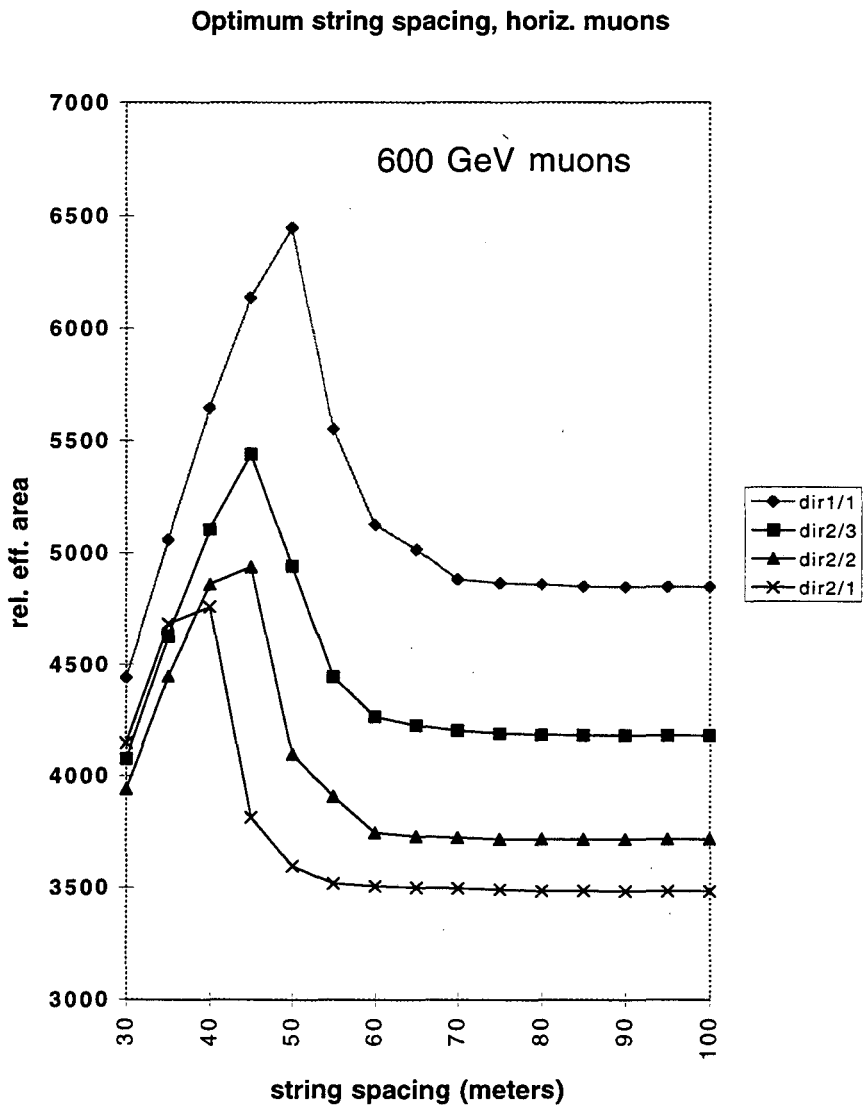**Optimum string spacing, horiz. muons**

Figure 13: The relative effective area (for 5 direct hits) obtained for 600 GeV muons incident horizontally (normal to a face) vs. the spacing between the strings. The calculations were made for a fixed OM spacing of 20 m. The maximum values of the respective curves indicate the optimum spacing for the different coincidence modes.
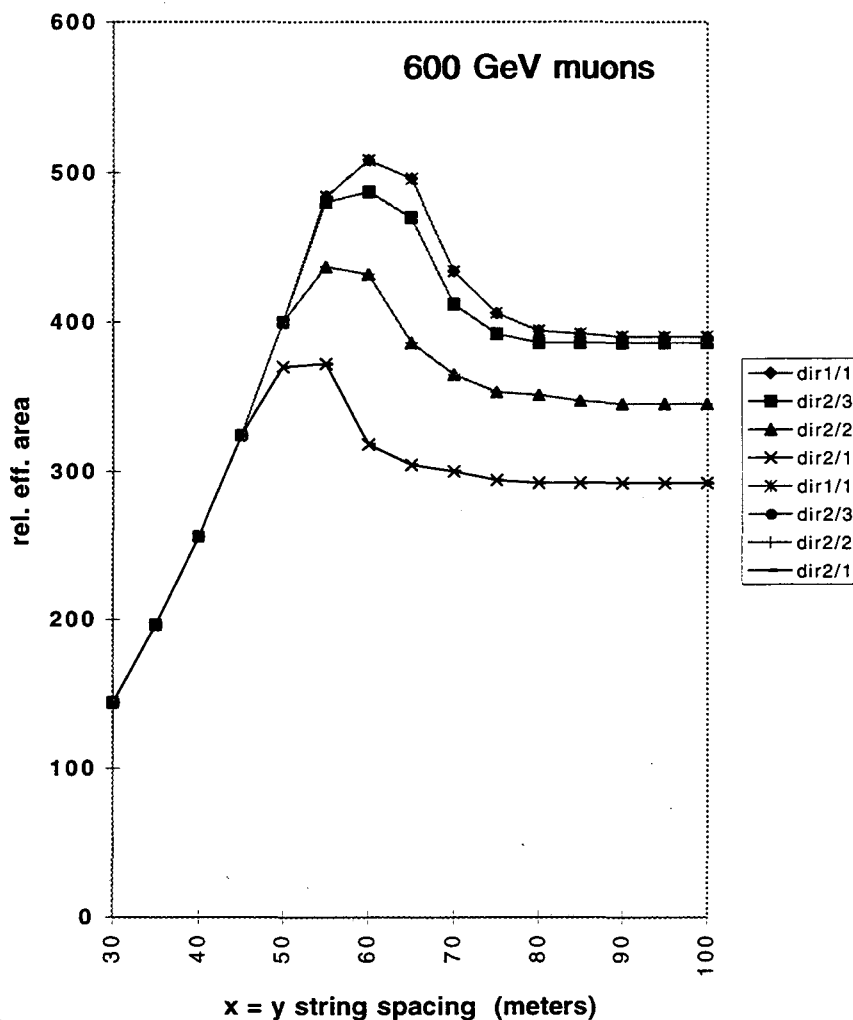
41

Figure 14: The relative effective area (for 5 direct hits) obtained for 600 GeV muons incident vertically upward vs. the spacing between the strings. The maximum values of the respective curves indicate the optimum spacing for the different coincidence modes.

Appendix B. Effective areas for arrays of other sizes

The changes in effective area when operating an array with a local coincidence depend on the parameters of the array. Here we present results for arrays having different string spacings and different numbers of OM's. This is by no means a systematic study and is intended only to give some idea of the variations one might expect.

Three other arrays are considered and included in Table B1 along with the particular array we have so far considered in detail. The thresholds used in calculating the effective areas are 16 ordinary hits and 5 directs hits. In all cases the vertical spacing between OM's is 20 meters, and the array is a $10x10$ rectangle having 100 strings. For these four cases the loss of effective area incurred in requiring a direct 2/3 coincidence (compared to the direct 1/1 singles) varies from 6% to 16 %. The dominant factor is the interstring spacing; the more optimal this spacing is for direct hits, the larger the effective area, even though the percentage loss in taking a local coincidence increases. Note that a 50 meter spacing is more optimal by 20-30 % for 600 GeV muons than is a 100 meter spacing. The number of OM's per string (20 versus 50) does not have much of an effect on the percentage loss of events associated with taking a local coincidence. Table B1 gives the effective areas for the four different array sizes and the ratio of the effective areas for the direct 2/3 and direct 1/1 modes. The third column is the geometric area of the illuminated side of the array.

Table B1

Effective areas for horizontal muons and arrays of different sizes. The third column is the geometrical area of one side. Units are km^2.

Spacing	OM's	geo.	1/1	2/3	2/2	2/1	dir1/1	dir2/3	dir2/2	dir 2/1	dir2/3 ÷ dir1/1
100m	5000	.88	.99	.65	.45	.26	.37	.34	.30	.27	0.94
50m	5000	.44	.56	.51	.49	.47	.48	.41	.34	.27	0.85
100m	2000	.34	.39	.24	.17	.10	.14	.13	.12	.11	0.92
50m	2000	.17	.23	.20	.19	.18	.19	.16	.13	.11	0.84

Acknowledgments

References

1. Physics capabilities of the second-stage Baikal detector NT-200
   Alatin S.D. et al., Nuclear Physics B (Proc.Suppl.), 1992, Vol.28A, 491.
   http://www.ifh.de/baikal/baikalhome.html

2. Technology Development for a Neutrino Astrophysical Observatory
   V. Chaloupka, et al., Lawrence Berkeley Laboratory Report LBL-38321, Feb. 1996.

3. Stage I R&D for a Km-Scale Neutrino Observatory: Detector Electronic Systems
   W. O. Chinowsky, et al., Proposal to the US DOE., Lawrence Berkeley National Laboratory, Feb. 1997.

4. Digital Optical Module & System Design Goals for 97-98
   D. Nygren and J. Przybylski, Lawrence Berkeley National Laboratory, Feb. 1998.

5. The AMANDA collaboration.
   http://amanda.berkeley.edu/www/amanda-events.html

6. Upgrade of AMANDA-B towards AMANDA-II
   A. Biron, et al., DESY-Zeuthen, A Proposal to DESY, PRC 97/05, June 1997.

7. Hit Probability and Energy Reconstruction in AMANDA
   C. Wiebusch, AMANDA Collaboration Meeting, Berkeley , Oct. 1997.

8. Bestimmung von Wasser- und Detektorparametern und Rekonstruktion von Myonen bid 100 TeV mit dem Baikal-Neutrinoteleskop NT-72
   D. Pandel Diplomarbeit, Feb. 1996.

9. Private communication from D. Pandel.

ERNEST ORLANDO LAWRENCE BERKELEY NATIONAL LABORATORY
ONE CYCLOTRON ROAD | BERKELEY, CALIFORNIA 94720